

Supplementary Information

Photocatalytic decomposition of hydrogen sulfide in Na₂SO₃ solution for hydrogen and value-added sulfur product over novel Ca-CdS Nanocrystals

Shan Yu,^{†b} Fan Wu,^{†b} Pengkun Zou,^b Xiang-Bing Fan,^c Chao Duan^b, Meng Dan,^{a,b} Zhanghui Xie,^b Qian Zhang,^{a,b} Fengying Zhang,^{a,b} Heng Zheng^d and Ying Zhou^{*a,b}

^a *State Key Laboratory of Oil and Gas Reservoir Geology and Exploitation, Southwest Petroleum University, Chengdu 610500, Sichuan, China*

^b *The Center of New Energy Materials and Technology, School of New Energy and Materials, Southwest Petroleum University, Chengdu 610500, Sichuan, China*

^c *Department of Engineering, University of Cambridge, Cambridge CB3 0FA, United Kingdom*

^d *State key laboratory of industrial vent gas reuse, Southwest Research & Design Institute of the Chemical Industry No. 87 Airport Road, Chengdu, Sichuan, China*

* Corresponding author Email addresses: yzhou@swpu.edu.cn (Y. Zhou), Fax: +86 28 83037406;

Tel: +86 28 83037401

† These authors contributed equally to this work.

TABLE OF CONTENT

Experimental	S3
Reaction mechanism of photocatalytic H₂S splitting	S6
Figure S1 The XRD patterns OF Ca-CdS NCs and CdS NCs.....	S7
Figure S2 TEM and HRTEM images of a-CdS NCs and CdS NCs.....	S8
Figure S3 XPS of Ca-CdS NCs and CdS NCs.....	S9
Figure S4 The long term test of H ₂ production over Ca-CdS NCs.....	S10
Figure S5 UV-Vis PL spectra of CdS NCs and Ca-CdS NCs.....	S11
Figure S6 TA and their respective SVD fitting for CdS NCs and Ca-CdS NCs.....	S12
Figure S7 EIS and transient photocurrent of CdS NCs and Ca-CdS NCs.....	S13
Figure S8 LSV of Na ₂ S/Na ₂ SO ₃ -H ₂ S solution and the solution with adding sulfur.....	S14
Figure S9 FT-IR spectra of different sulfur-containing chemicals.....	S15
Figure S10 FT-IR spectra of the products over other photocatalysts.....	S16
Figure S11 The XRD and photograph of final oxidation product.....	S17
Figure S12 UV-Vis absorption spectra of photocatalytic reaction solution.....	S18
Table S1 ICP-AES of the CdS NCs and Ca-CdS NCs.....	S19
Table S2 Content of Cd before and after synthesis of Ca-CdS NCs in the solution	S20
Table S3 Zeta potential of the CdS NCs and Ca-CdS NCs.....	S21

Table S4 H ₂ evolution results over the Na ₂ SO ₃ solution with different treatment.....	S22
Table S5 The pH value and concentration of H ₂ S about different reaction medias.....	S23
References	S24

Experimental

Materials

Sodium sulfide ($\text{Na}_2\text{S}\cdot 9\text{H}_2\text{O}$, $\geq 98\%$), sodium sulfite (Na_2SO_3 , 97%), sodium sulphate (Na_2SO_4 , 99%), Potassium persulfate ($\text{K}_2\text{S}_2\text{O}_8$, 99.5%), hydrochloric acid (HCl, 36%-38%), potassium iodide (KI, 99.0%), Iodine (I_2 , 99.8%) and calcium nitrate tetrahydrate ($\text{Ca}(\text{NO}_3)_2\cdot 4\text{H}_2\text{O}$, 99%) were purchased from Chron Chemicals (Chengdu, China). Sodium thiosulfate pentahydrate ($\text{Na}_2\text{S}_2\text{O}_3\cdot 5\text{H}_2\text{O}$, 99.99%), cadmium chloride hemi (pentahydrate) ($\text{CdCl}_2\cdot 2.5\text{H}_2\text{O}$, 99%), Cadmium Sulfide (CdS, 99.999%), acetate (CH_3COOH , 99.7%) and formaldehyde (HCHO, 37%-40%) was obtained from Aladdin (Shanghai, China). All of the materials were used as received without further purification.

Characterization

The crystal structure and crystallinity of the samples were studied by X-ray diffraction (XRD) with Cu K α radiation using Philips X'Pert diffractometer at 40 kV and 40 mA. UV-vis absorption spectra and diffuse reflection spectra (DRS) were recorded with a Shimadzu UV-2600 spectrophotometer. Morphology of NCs were studied using a transmission electron microscope (TEM, FEI TECNAI G2S-TWIN). energy dispersive X-ray spectroscopy (EDS) were performed on a JEOL JSM-7800F microscopy equipped with EDAX detector. X-ray photoelectron spectra (XPS) were obtained by Thermo Fisher Scientific ESCALAB 250Xi X-ray photoelectron spectrometer and all of the binding energies were referenced to the C 1s level at 284.8 eV. Steady-state Photoluminescence spectra (PL) was recorded with an Edinburgh FLS1000 fluorescence spectrophotometer. Zeta potential of the samples was measured by a Brookhaven Zeta PALS 190 Plus analyzer. Photoelectrochemical activity was measured via CHI660E electrochemical work station (Chenhua Instrument, Shanghai, China) with a standard three-electrodes system (counter electrode: Pt, reference electrode: saturated calomel electrode). The elements in the composites were determined by inductively coupled plasma atomic emission spectrometry (ICP-AES, Varian ES) after the samples were dissolved in a mixture solution of HNO_3 and HCl. The Fourier-transform infrared (FT-IR) spectra were studied on a Bruker infrared spectrometer (Tensor II) on samples embedded in KBr pellets.

Synthesis of CdS NCs and Ca-CdS NCs

The synthesis of CdS NCs and Ca-CdS NCs were derived from the literature report with some

modification.^[1] For synthesis of Ca-CdS NCs, 55 mL aqueous solution contain 114 mg (0.5 mmol) $\text{CdCl}_2 \cdot 2.5\text{H}_2\text{O}$ was heated to 80 °C in a 100 mL three-neck flask under an inertia environment and continuous stirring. And then, a freshly prepared 5 mL Na_2S solution containing 600 mg (2.5 mmol) $\text{Na}_2\text{S} \cdot 9\text{H}_2\text{O}$ was rapidly injected the above solution. The reaction was maintained at 80 °C for 2 h with stirring and under argon atmosphere to obtain an orange-yellow precipitates. Then precursor Ca^{2+} (5 mL water with 59 mg (0.25 mmol) $\text{Ca}(\text{NO}_3)_2 \cdot 4\text{H}_2\text{O}$) was slowly dropped into the reaction solution within 10 min. After that, the obtained mixture was retained at 80 °C for another 1 h. The NCs was then collected by centrifugation, washed with ethanol/water to get rid of any unreacted ions, and finally dispersed in water by ultrasound.

The process of synthesis of CdS NCs was much similar to the synthesis of Ca-CdS NCs above with directly heating for 3 h at 80 °C but without Ca^{2+} precursor additionally introduced in the three-neck flask.

Linear sweep voltammetry experiments

The linear sweep voltammogram (LSV) of different reaction medias was performed from literature reported with some modification.^[2] Simply, a standard three-electrode electrochemical system was applied for linear sweep voltammetry and cyclic voltammetry measurement. The platinum patch was used as working and counter electrode and an SCE used as the reference electrode. The scan rate was 50 mV/s, and all measurements were via CHI660E electrochemical work station (Chenhua Instrument, Shanghai, China) at room temperature. The electrolyte contained $\text{Na}_2\text{S}/\text{Na}_2\text{SO}_3\text{-H}_2\text{S}$ or $\text{Na}_2\text{SO}_3\text{-H}_2\text{S}$ solution was kept under continuous magnetic stirring during the measurements.

Transient absorption

Transient absorption (TA) spectra were implemented based on standard pump-probe setup.^[3] Briefly, laser pulses (800 nm, 120 fs pulse length, 1 kHz repetition rate) were generated by a regenerative amplifier (Spitfire XP Pro) seeded by a femtosecond oscillator (Tsunami, both Spectra-Physics). Excitation pulses at a wavelength of 400 nm were generated by a BBO crystal and to be as a second harmonic of the laser. The super-continuum probe laser we used came from a thin CaF_2 plate. The polarization angle of 54.7° between pump and probe beams was achieved by placing a Berek compensator in the pump beam. To avoid photodamage of samples, they were moved constantly after each time delay point.

Calculation of hydrogen sulfide Concentration

The concentration of H₂S in the alkaline solution, approximately equal to HS⁻ concentration in the solution, was detected by the ultraviolet visible spectrophotometry. The concentration is linearly proportional to the absorbance according to the Beer-Lambert law $A = \epsilon \times b \times C$ where A, ϵ , b, C are absorbance of the solution, molar absorptivity, path length, and solution concentration, respectively, in which ϵ and b are constant.^[4, 5] Thus, the concentration of HS⁻ can be found by measuring absorbance of the solution by UV-Vis at the wavelength of 232 nm. First, standard curve of the concentration about HS⁻ was fabricated shown at the Eq. (1), where the $C_{[HS^-]}$, constant 0.1316 represents the concentration of HS⁻ and the slope of the fitting plot ($R^2=0.9979$), respectively.

$$C_{[HS^-]} = 0.1316 \times A \quad (1)$$

The absorbance of the reaction system after H₂S bubbling was measured by UV-visible spectrophotometer over the supernatant fluid after adding BaCl₂ to precipitate SO₃²⁻ in the solution. Finally, the HS⁻ concentration was obtained according to Eq. (1).

Photocatalytic H₂ evolution from H₂S

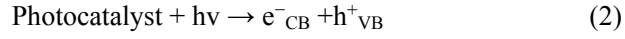
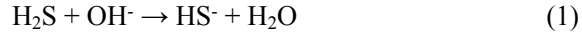
The photocatalytic H₂ evolution from H₂S with nanocrystal were conducted in a home-made setup.^[6] At first, H₂S gas was produced by dropwise addition of 150 mL Na₂S solution (1 M) to 150 mL HCl solution (2 M), which was then continuously bubbled into three-neck flask containing 50 mL 0.6 M Na₂SO₃ to form H₂S absorbent. A Pyrex tube with 1 mg of NCs, 5 mL of H₂S absorbent and 0.5 mL CH₄ as internal standard for quantitative analysis of the amount of H₂ was then illuminated by monochromatic LED light (460 nm, 3 W) with constant stirring and water circulation cooling. The amount of produced H₂ was confirmed by gas chromatograph (TM GC-2010 Plus, China, Ar carrier gas, molecular sieve 5 Å, TCD detector).

Quantitative analysis of thiosulfate

The quantitative analysis of the amount of thiosulfate (S₂O₃²⁻) in the reaction solution was performed by the iodometry method. Typically, the reaction solution was firstly diluted by 10 times, and then S²⁻ was removed from the system by addition of excessive CdCl₂·2.5H₂O and filtration. Furthermore, 10 mL of formaldehyde was adopted as the mask agent for SO₃²⁻ and the solution was adjusted to weakly acidic with 10 mL 10% acetate buffer solution. After that, 1 mL starch indicator was added, and then the obtained solution titrated with iodine standard solution (0.1 M). Result was obtained based on three repeated independent measurements.

Reaction mechanism of photocatalytic H₂S splitting

The mechanism for photocatalytic H₂S splitting in Na₂SO₃ solution can be described as following:^[6]



HS⁻ was firstly produced in the basic Na₂SO₃ solution after introduction of H₂S (Eq. 1). Photogenerated holes from valence band of Ca-CdS NCs under light irradiation were effectively consumed by HS⁻ to generate hydrogen ions and sulfur, and the reduction of protons took place simultaneously by photogenerated electrons on the conduction band of Ca-CdS NCs (Eqs. 2-4). And then SO₃²⁻ reacted with sulfur on the catalysts surface to avoid the deposition of S and endowed the long-time activity for hydrogen evolution (Eq. 5). Overall, an efficient photocatalytic H₂S splitting system can be achieved in Na₂SO₃ solution with Ca-CdS NCs.

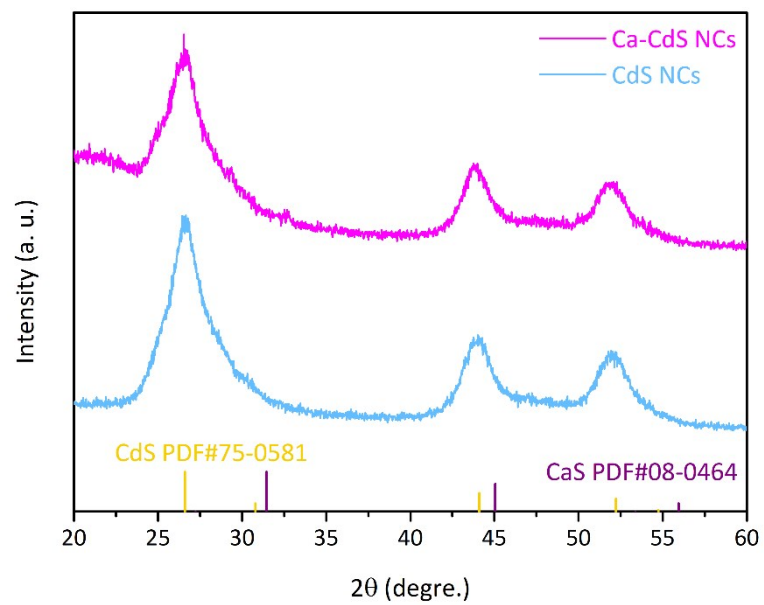


Figure S1 The XRD patterns of Ca-CdS NCs and CdS NCs.

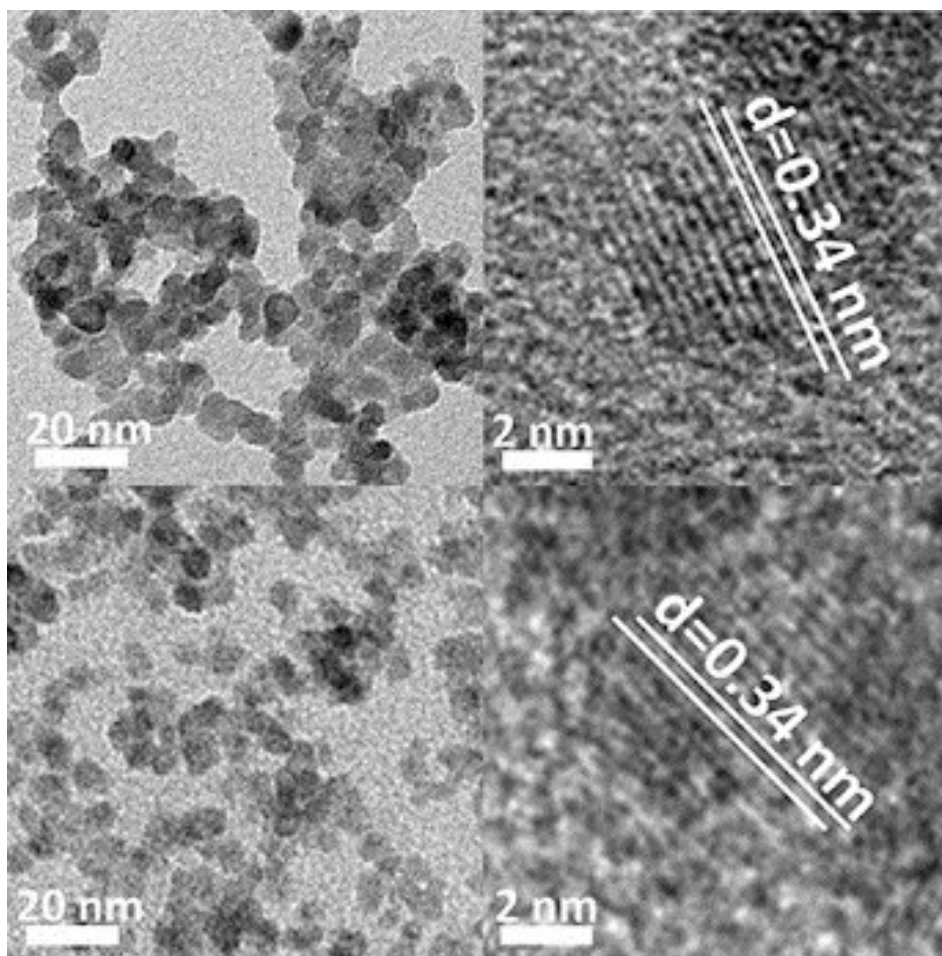


Figure S2 Transmission electron microscopy (TEM) and high-resolution TEM (HRTEM) images of CdS NCs (a, b), Ca-CdS NCs (c, d).

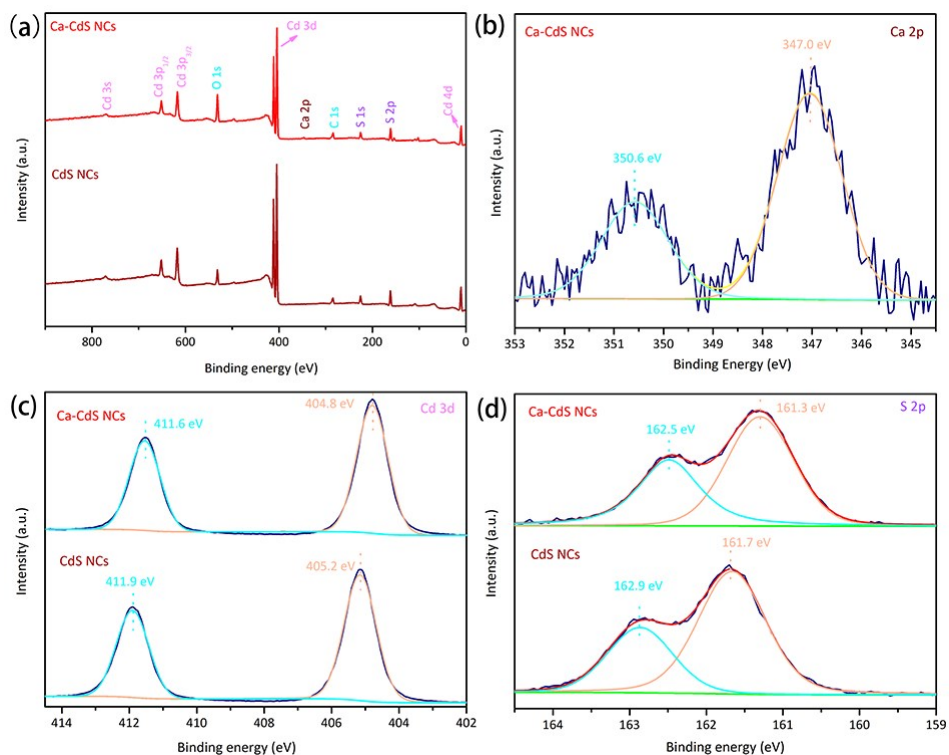


Figure S3 X-ray photoelectron spectra (XPS) of Ca-CdS NCs and CdS NCs. Survey (a), Ca 2p (b), Cd 3d (c), S 2p (d).

Element compositions and chemical information of the as-prepared samples were further analyzed by XPS in view of distinct electron binding energy of calcium, cadmium and sulfur. The XPS survey scan confirmed the existence of Ca elements for Ca-CdS NCs compared to CdS NCs in Fig. 3a.^[7,8] And the Ca 2p 3/2 and 2p 1/2 peaks were located at 347.0 eV and 350.0 eV (Fig. 3b), respectively, which were consistent with those reported Ca²⁺.^[7] The binding energies of S 2p 3/2 and 2p 1/2 are identified at 161.7 and 162.9 eV, corresponding to the valence state of S²⁻. The two peaks of Cd 3d 5/2 and 3d 3/2 located at 405.2 and 411.9 eV with a splitting energy of 6.7 eV finely assigned to the Cd²⁺ in CdS NCs (Fig. 3d).^[8]

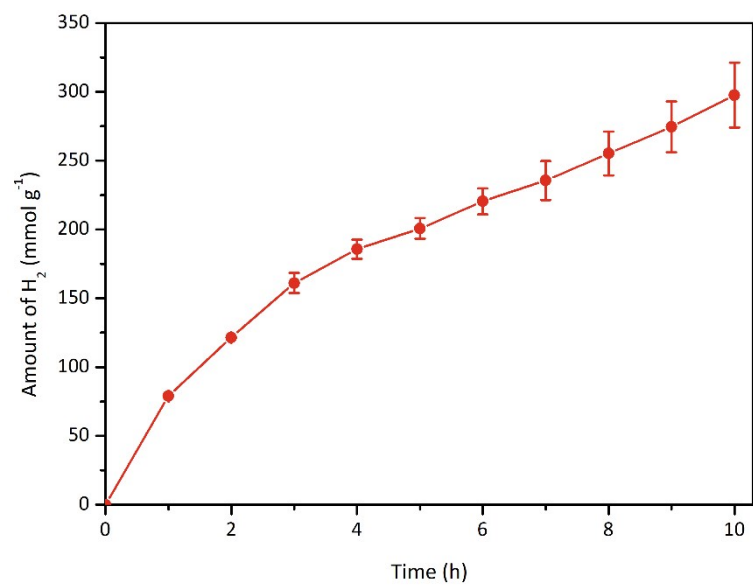


Figure S4 The long term test of H_2 production over Ca-CdS NCs. Reaction condition: 5 mL 0.6 M Na_2SO_3 - H_2S solution with 1 mg Ca-CdS NCs illuminated by 460 nm LED light.

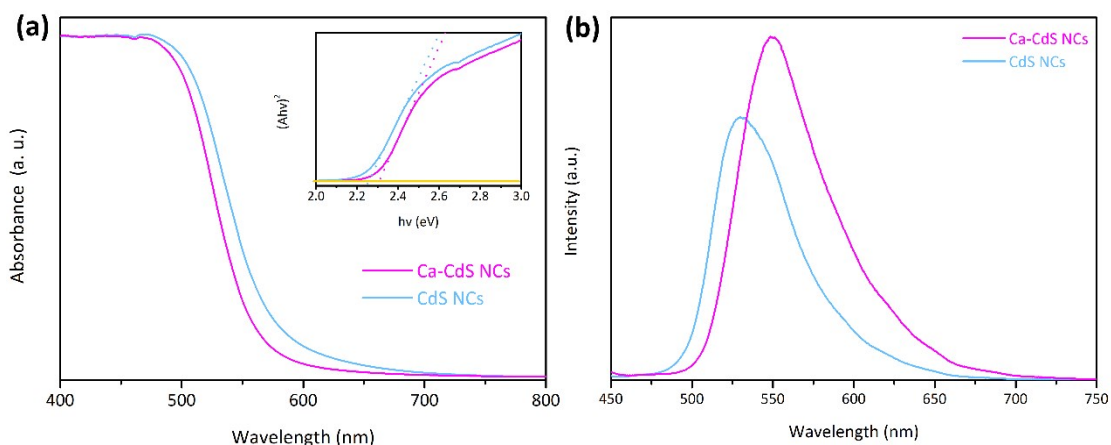


Figure S5 UV-Vis absorption (a) and steady state photoluminescence (PL) spectra (b) of CdS NCs and Ca-CdS NCs. PL was subsequently measured in same concentration calibrated by ICP with excitation wavelength at 400 nm. Inset: Tauc plots for each sample showing indirect band gaps.

The nanocrystals' luminescence emission mainly contains band-edge emission and trap emission. Among them, the band-edge emission is related to radiative recombination between conduction band and valence band, and the emission wavelength is slightly longer than their UV-Vis absorption peak; and trap-state emission is originated from trap states, with an obviously longer wavelength than that with the band gap emission.^[9] Band-edge emission intensity is inversely proportional to the number of defects, and trap-state emission is directly proportional to the number of defects. For the Ca-CdS NCs, the peak of PL emission is around 550 nm that is close to the UV-Vis absorption edge (521 nm), which indicates the luminescence of NCs is band-edge emission.^[10-12] Hence, the higher PL intensity of NCs means the band-edge emission was strengthened by modifying Ca^{2+} , which indicated defects in NCs surface were efficiently passivated.

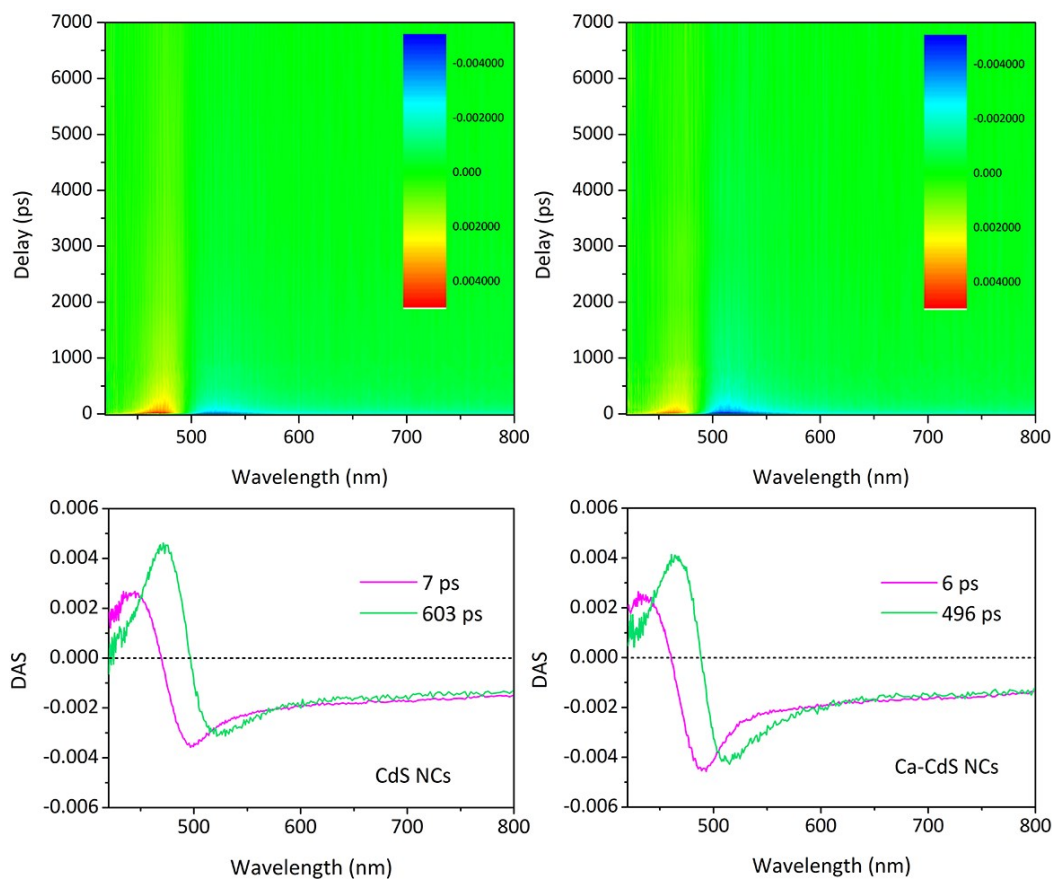


Figure S6 TA spectra with 400 nm excitation (2×10^{12} ph/cm²/pulse) and (c, d) their respective SVD fitting for CdS NCs and Ca-CdS NCs.

According to transient absorption (TA) results, the distinct ground-state bleach signals located at 500 nm for both NCs are caused by the state filling of the conduction band electron. For two decay components from the singular value decomposition (SVD) fitting, there's no obvious difference for the fast components at fs scale, but Ca-CdS NCs showed faster non-radiative process with lifetimes of 496 ps than CdS NCs (603 ps), and the closer Gaussian distribution decay curve in Ca-CdS NCs reconfirmed their fewer defects.

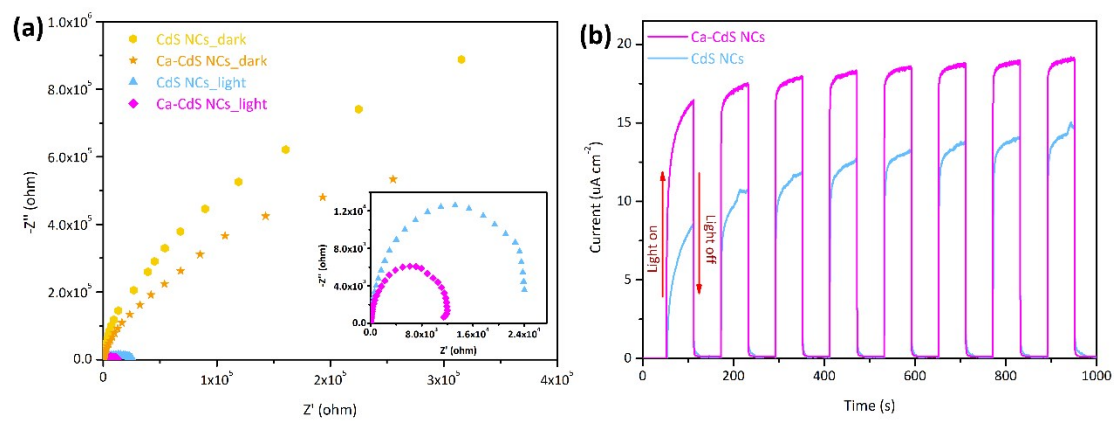


Figure S7 Electrochemical impedance spectra (EIS) (a) and transient photocurrent scans (b) of CdS NCs and Ca-CdS NCs. The photoelectrochemical measurements over all the samples were tested under visible-light irradiation ($\lambda > 420$ nm) with 1.2 M Na_2SO_3 solution as the electrolyte. Inset of (a) is the enlargement of the EIS of NCs.

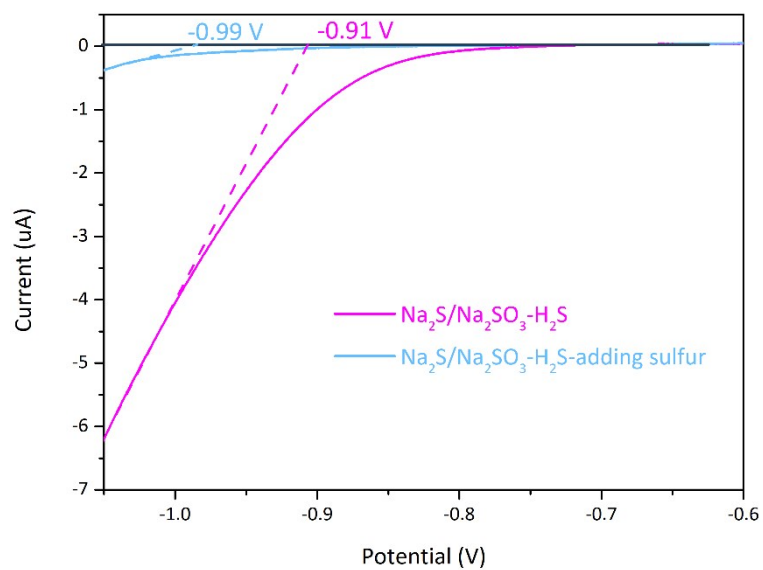


Figure S8 Linear sweep voltammograms (LSV) of Na₂S/Na₂SO₃-H₂S solution and the solution with adding sulfur. All the tests were performed under a scan rate of 50 mV s⁻¹ at room temperature with platinum as working and counter electrode and SCE as reference.

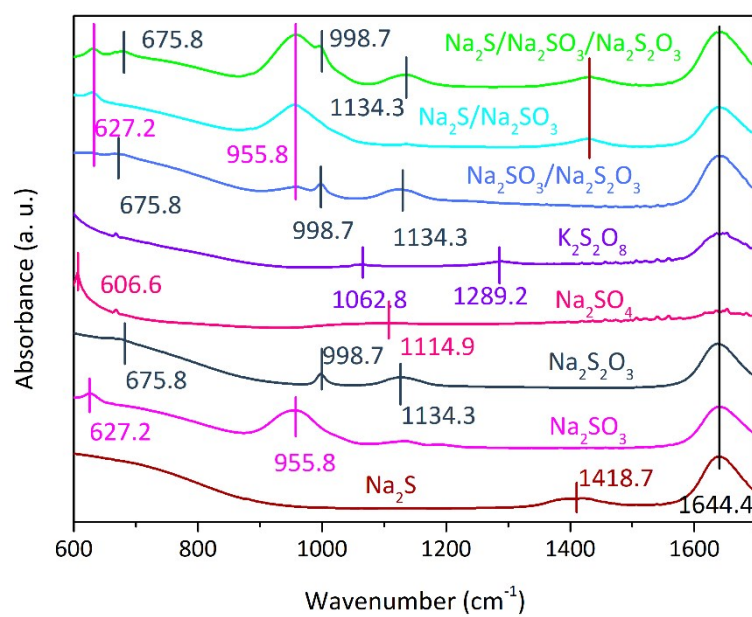


Figure S9 FTIR spectra of different sulfur-containing chemicals. The strong band appeared at 1644.4 cm⁻¹ can contribute to the presence of liquid water on the surface of samples.^[13]

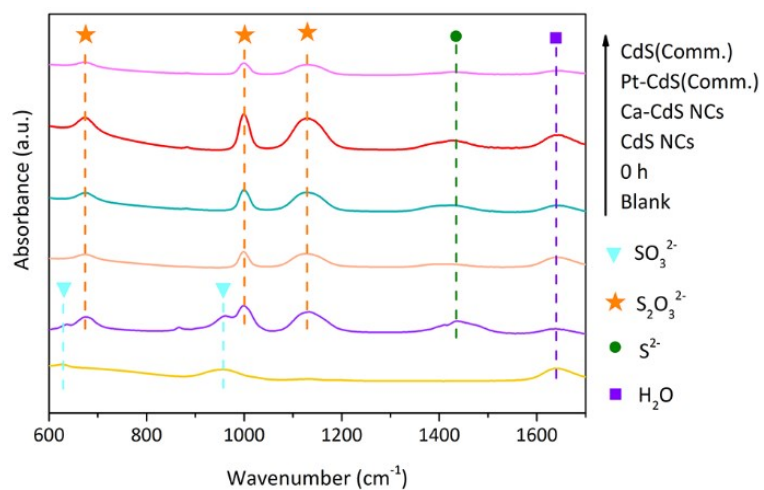


Figure S10 FT-IR of the product after photocatalytic reaction 3 h in the Na₂SO₃-H₂S solution with CdS NCs, Ca-CdS NCs, pristine commercial CdS (CdS(Comm.)) and Pt-loaded commercial CdS (Pt-CdS(Comm.)) as photocatalyst. Blank means pure Na₂SO₃ solution without H₂S.

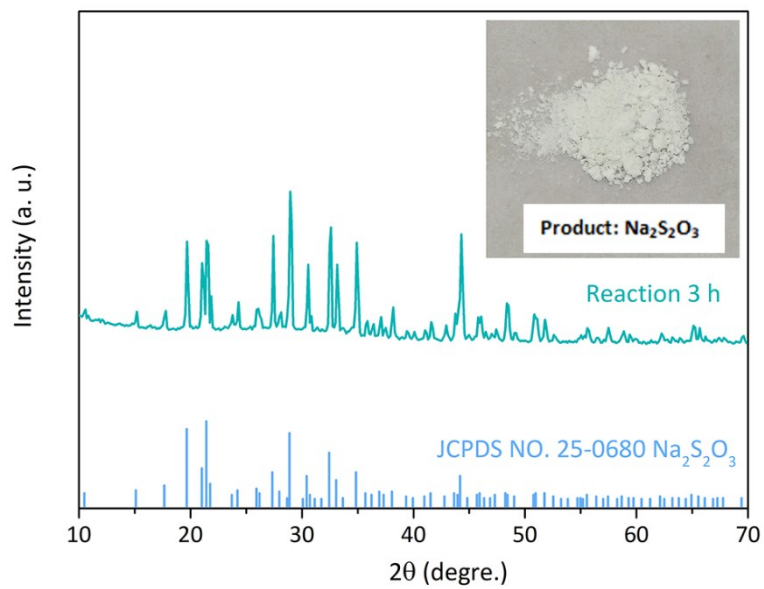


Figure S11 The XRD and photograph of reaction product after photocatalysis. The product was collected by evaporation and drying of the reaction solution at 50 °C under Ar atmosphere.

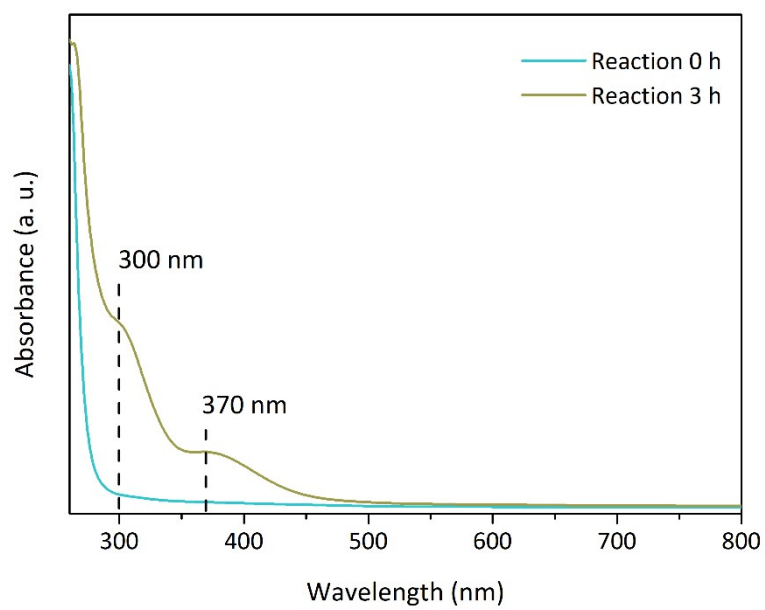


Figure S12 UV-Vis absorption spectra of the photocatalytic reaction solution diluted by 10 times.

Table S1 ICP-AES of the CdS NCs and Ca-CdS NCs

	Cd	Ca
CdS NCs	61.8 wt%	-
Ca-CdS NCs	60.7 wt%	7.5 wt%

Table S2 Content of Cd before and after synthesis of Ca-CdS NCs in the solution

Content	Cd (mmol)
Before synthesis (C_1)	0.5
After synthesis (C_2)	0.5×10^{-3}

Note: The amount of Cd in the solution before synthesis was determined by the addition amount of Cd precursor in the system, and that after synthesis is determined by ICP-AES measurement.

Table S2 shows the amount of Cd in solution before and after synthesis of Ca-CdS NCs. It turns out the amount of Cd in the supernatant of Ca-CdS NCs is only 0.5×10^{-3} mmol, which only accounts 0.1% to the total amount of Cd (0.5 mmol, calculated from the precursor) in the reaction system. Therefore, it is inferred that 99.9% of Cd precursor successfully grew into Ca-CdS NCs and hence the possibility of cation exchange between Ca^{2+} and Cd^{2+} for formation of solid solution is very small.

Table S3 Zeta potential of the CdS NCs and Ca-CdS NCs

	CdS NCs	Ca-CdS NCs
Zeta potential (mV)	-29.1 ± 0.4	-16.0 ± 0.6

Table S4 Photocatalytic H₂ production over Ca-CdS NCs in 0.6 M Na₂SO₃ solution as reaction media with different treatment

Reaction solution	pH	H ₂ production (mmol g ⁻¹ h ⁻¹)
0.6 M Na ₂ SO ₃ -H ₂ S	7.55	56.0
0.6 M Na ₂ SO ₃ -H ₂ O	10.60	4.85
0.6 M Na ₂ SO ₃ -H ₂ O-Na ₂ S/HCl	7.60	10.2
0.6 M Na ₂ SO ₃ -H ₂ O-HCl	7.65	14.3
No light ^a	7.55	trace
No catalysts ^a	7.55	trace

a: Reaction at 0.6 M Na₂SO₃ aqueous solution with 0.24 M H₂S. Reaction condition: 5 mL reaction solution, 1 mg Ca-CdS NCs and 460 nm LED light.

Table S5 The pH value and concentration of H₂S about different reaction medias at various reaction terms

pH	Before H ₂ S gas	Reaction 0 h	C(H ₂ S)
0.6 M Na ₂ SO ₃	10.60	7.55	0.42 M
0.5 M KOH	13.34	7.65	0.3 M
0.6 M Na ₂ SO ₃ /0.1 M Na ₂ S	13.35	7.60	0.24 M

References

- [1] X.-B. Fan, S. Yu, H.-L. Wu, Z.-J. Li, Y.-J. Gao, X.-B. Li, L.-P. Zhang, C.-H. Tung, L.-Z. Wu, *J. Mater. Chem. A*, **2018**, *6*, 16328-16332.
- [2] G.J. Ma, H.J. Yan, J.Y. Shi, X. Zong, Z.B. Lei, C. Li, *J. Catal.*, **2008**, *260*, 134-140.
- [3] F.Y. Zhou, *J.S. chem*, Y. Zhou, R.X. He, K.B. Zheng, *J. Lumin.*, **2020**, *220*, 117023.
- [4] M.R. Bayati, A.Z. Moshfegh, F. Golestani-Fard, *Appl. Catal. A: Gen.*, **2011**, *389*, 60-67.
- [5] L.M. Levchenko, A.A. Galitskii, V.V. Kosenko, A.K. Sagidullin, *Russ. J. Appl. Chem.*, **2015**, *88*, 1403-1408.
- [6] M. Dan, A. Prakash, Q. Cai, J.L. Xiang, Y.H. Ye, Y. Li, S. Yu, Y.H. Lin, Y. Zhou, *Solar RRL*, **2019**, *3*, 1800237.
- [7] J.J. Ding, S. Sun, W.H. Yan, J. Bao, C. Gao, *Int. J. Hydrogen Energy*, **2013**, *38*, 13153-13158.
- [8] Z.J. Sun, H.F. Zheng, J.S. Li, P.W. Du, *Energy Environ. Sci.*, **2015**, *8*, 2668-2676.
- [9] H. Hsiu-Y. Wei, C.M. Evans, B.D. Swartz, A.J. Neukirch, J. Young, O.V. Prezhdo, T.D. Krauss, *Nano Lett.*, **2012**, *12*, 4465-4471.
- [10] C.B. Murray, D.J. Norris, M.G. Bawendi, *J. Am. Chem. Soc.*, **1993**, *115*, 8706-8715;
- [11] W.W. Yu, X.G. Peng, *Angew. Chem. Int. Ed.*, **2002**, *41*, 2368-2371;
- [12] S. Yu, X.-B. Fan, X. Wang, J.G. Li, Q. Zhang, A.D. Xia, S.Q. Wei, L.-Z. Wu, Y. Zhou, G.R. Patzke, *Nat. Comm.*, **2018**, *9*, 4009.
- [13] J. Yota, V.A. Burrows, *J. Vac. Sci Technol. A*, **1993**, *11*, 1083-1088.